

Microscopic insight into the origin of enhanced glass-forming ability of metallic melts on micro-alloying

C. J. Chen, A. Podlesnyak, E. Mamontov, W. H. Wang, and S. M. Chathoth

Citation: *Applied Physics Letters* **107**, 131901 (2015); doi: 10.1063/1.4932049

View online: <http://dx.doi.org/10.1063/1.4932049>

View Table of Contents: <http://scitation.aip.org/content/aip/journal/apl/107/13?ver=pdfcov>

Published by the **AIP Publishing**

Articles you may be interested in

[Unique properties of CuZrAl bulk metallic glasses induced by microalloying](#)

J. Appl. Phys. **110**, 123522 (2011); 10.1063/1.3672449

[Enhancement of glass-forming ability and corrosion resistance of Zr-based Zr-Ni-Al bulk metallic glasses with minor addition of Nb](#)

J. Appl. Phys. **110**, 023513 (2011); 10.1063/1.3606642

[Enhanced glass-forming ability of FeCoBSiNb bulk glassy alloys prepared using commercial raw materials through the optimization of Nb content](#)

J. Appl. Phys. **107**, 09A315 (2010); 10.1063/1.3350898

[A criterion for evaluating glass-forming ability of alloys](#)

J. Appl. Phys. **106**, 094902 (2009); 10.1063/1.3255952

[Highly processable bulk metallic glass-forming alloys in the Pt-Co-Ni-Cu-P system](#)

Appl. Phys. Lett. **84**, 3666 (2004); 10.1063/1.1738945



MMR TECHNOLOGIES

**THE WORLD'S RESOURCE FOR
VARIABLE TEMPERATURE
SOLID STATE CHARACTERIZATION**

WWW.MMR-TECH.COM

OPTICAL STUDIES SYSTEMS SEEBECK STUDIES SYSTEMS MICROPROBE STATIONS HALL EFFECT STUDY SYSTEMS AND MAGNETS

Microscopic insight into the origin of enhanced glass-forming ability of metallic melts on micro-alloying

C. J. Chen,¹ A. Podlesnyak,² E. Mamontov,³ W. H. Wang,⁴ and S. M. Chathoth^{1,a)}

¹Department of Physics and Materials Science, City University of Hong Kong, Kowloon Tong, Hong Kong, People's Republic of China

²Quantum Condensed Matter Division, Oak Ridge National Laboratory, Oak Ridge, Tennessee 37831, USA

³Chemical and Engineering Materials Division, Oak Ridge National Laboratory, Oak Ridge, Tennessee 37831, USA

⁴Institute of Physics, Chinese Academy of Science, Beijing 100190, People's Republic of China

(Received 24 August 2015; accepted 17 September 2015; published online 28 September 2015)

Extensive efforts have been made to develop metallic-glasses with large casting diameter. Such efforts were hindered by the poor understanding of glass formation mechanisms and the origin of the glass-forming ability (GFA) in metallic glass-forming systems. In this work, we have investigated relaxation dynamics of a model bulk glass-forming alloy system that shows the enhanced at first and then diminished GFA on increasing the percentage of micro-alloying. The micro-alloying did not have any significant impact on the thermodynamic properties. The GFA increasing on micro-alloying in this system cannot be explained by the present theoretical knowledge. Our results indicate that atomic caging is the primary factor that influences the GFA. The composition dependence of the atomic caging time or residence time is found to be well correlated with GFA of the system. © 2015 AIP Publishing LLC. [<http://dx.doi.org/10.1063/1.4932049>]

Extensive research efforts have been taken to develop metallic-glasses with large casting diameter. Such efforts are impeded by the poor understanding of glass formation mechanisms and the factors influencing the glass-forming ability (GFA) of metallic glass-forming systems.^{1–3} Recently, it was discovered that the GFA of certain alloys dramatically increases by the use of micro-alloying.⁴ The micro-alloying did not have any significant impact on the thermodynamic parameters such as the crystallization (T_x) and melting temperature (T_m) or the glass-transition temperature (T_g) of the alloys.⁴ The phenomena of increasing GFA on micro-alloying cannot be explained by the often-cited empirical rules for the metallic glass formation: that the alloy should be a multicomponent system where atomic size ratios should be above 12%, the negative heat of mixing of components, and the deep eutectic rule based on the T_{rg} criterion.^{5,6} In general, when a liquid is cooled below the melting temperature, it crystallizes. During crystallization, atoms in the liquid undergo a highly correlated set of motions. If the highly correlated atomic motions are retarded, then a disordered structure will be formed. Thus, GFA could be related to the factors that hinder the ability of correlated motions. Therefore, a fundamental understanding of vitrification mechanism as well as GFA requires the knowledge of atomic dynamics of the glass-forming liquids.

In this work, we have investigated the atomic dynamics of Ce based bulk glass-forming alloy melts by quasi-elastic neutron scattering (QENS). The Ce based bulk glass-forming alloys show increased casting thickness with micro-alloying Co. The $\text{Ce}_{70}\text{Cu}_{20}\text{Al}_{10}$ is a bulk glass-forming alloy with a very low glass-transition temperature, and it can be cast into 2 mm diameter rods. By the addition of Co in very small

percentage, the critical casting thickness is found to be increased. The addition of just 0.2 at. % Co increases the critical casting diameter from 2 to 8 mm. Further addition of Co at 1% to 2% increased the casting thickness up to 10 mm. However, above 2%, addition of Co decreases the casting thickness of $\text{Ce}_{70}\text{Cu}_{20}\text{Al}_{10}$ alloy. Thus, the GFA of $\text{Ce}_{70}\text{Cu}_{20}\text{Al}_{10}$ alloy at first increases and then decreases with Co addition. There is no dramatic shift in the T_g , T_x , and T_l temperatures of the micro-alloyed samples. The reduced glass-transition temperature, which is a thermodynamic measure of GFA, increased from 0.470 ($\text{Ce}_{69.8}\text{Cu}_{20}\text{Al}_{10}\text{Co}_{0.2}$) to 0.492 ($\text{Ce}_{68}\text{Cu}_{20}\text{Al}_{10}\text{Co}_2$).⁴ Therefore, these Ce based alloys are the excellent class of materials to understand the influence of atomic dynamics on GFA.

The alloys were prepared by arc melting of pure elements, Ce (99.5%), Cu(99.99%), Al(99.99%), and Co (99.99%). The alloy samples were then powered and remelted in Al_2O_3 crucibles under high vacuum. The Al_2O_3 crucibles provide a hollow cylindrical geometry to the sample with 2 mm thickness, 22 mm width, and 40 mm height. The QENS experiments were done on Cold Neutron Chopper Spectrometer (CNCS) at the Spallation Neutron Source, Oak Ridge, U.S.A.⁷ We have selected a neutron wavelength of 3.6 Å, which provides a momentum transfer range of 0.3–2.8 Å⁻¹ and an energy resolution of 160 μeV (full-width at half-maximum of the Vanadium standard data measured at room temperature). The samples were measured at five different temperatures; starting from 850 K to 1250 K, in steps of 100 K. Many inelastic neutron scattering experiments have shown that even for the samples composed of the elements that scatter neutrons predominantly coherently, at low Q values (below the first structure factor maximum) the incoherent contribution to the scattering intensity becomes significant.^{8–10} The first structure factor maximum of the present alloy melts is found at a Q value of 2.8 Å⁻¹, so for

^{a)}Author to whom correspondence should be addressed. Electronic mail: smavilac@cityu.edu.hk

the data analysis the Q range was restricted to $0.3\text{--}2.0\text{ \AA}^{-1}$. Therefore, at this low Q range, the scattered signals are dominated by the incoherent contributions from the Cu atoms. The data were collected over a period of 4 h at each temperature. An empty sample container was also measured at each temperature to eliminate its contribution to the scattered signals. A vanadium foil with similar sample geometry was used to normalize the scattering signals. The dynamic structure factors $S(Q, \omega)$ were obtained by correcting for self-absorption and container scattering, interpolating to constant Q , and symmetrizing with respect to the detailed balanced factor. The $S(Q, \omega)$ were then Fourier transformed into the time space, deconvolved from (i.e., divided by) the instrument resolution function, and normalized to unity to obtain the self-correlation functions $\Phi(Q, t)$.

Fig. 1 shows the $\Phi(Q, t)$ of $\text{Ce}_{68}\text{Cu}_{20}\text{Al}_{10}\text{Co}_2$ measured at different temperatures. The $\Phi(Q, t)$ decays non-exponentially with time and can be well fitted with a *Kohlrausch–Williams–Watts* (KWW) function as follows:

$$\Phi(Q, t) = f_Q \exp(-t/\tau_Q)^\beta. \quad (1)$$

Here, f_Q is the Debye-Waller factor, τ_Q is the relaxation time, and β is the stretching exponent. The value of β was found to be independent of composition and temperature, but varying with Q , that is, decreasing systematically from 0.9 to 0.7 over the Q range of 0.3 to 2.0 \AA^{-1} . The stretching of the self-correlation function is normally observed in fragile glass-forming liquids, and the value of β was found to be related to the fragility of the liquids.¹¹ Highly fragile liquids exhibit smaller values for β (larger stretching), whereas strong liquids show larger values for β . In the present case, there is no significant change in the fragility of the liquids as a function of temperature and composition. The value of β was found to be almost constant and comparable to the previous results.¹² On the other hand, the observed variation of stretching exponent with Q values might be due to the heterogeneous nature of the dynamics present in the alloy liquids. The mean relaxation times were calculated from the relaxation time parameters obtained from the KWW fitting using the following equation: $(\tau_Q) = \tau_Q \beta^{-1} \Gamma(\beta^{-1})$, where Γ is the

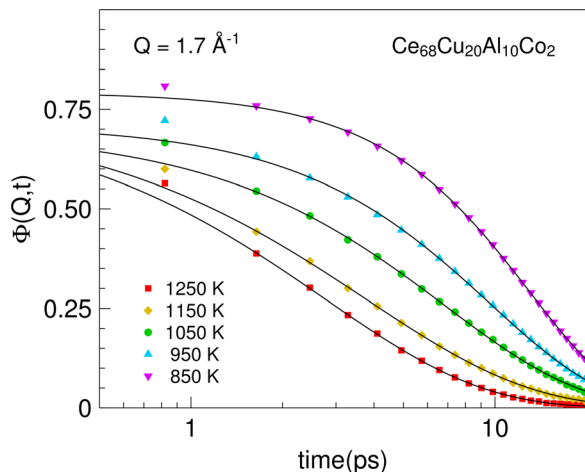


FIG. 1. The self-correlation function of Cu atoms in $\text{Ce}_{68}\text{Cu}_{20}\text{Al}_{10}\text{Co}_2$ alloy melt at different measured temperatures at a Q value of 1.70 \AA^{-1} . The solid lines are fits with KWW function (Eq. (1)).

gamma function. The mean relaxation times were plotted as a function of the square of momentum transfer in Fig. 2. The relaxation time follows a straight line path in the hydrodynamic regime, that is, at Q values well below the static structure factor maximum. For a long range atomic diffusion process, the mean relaxation times are proportional to Q^2 in the hydrodynamic regime.⁹ However, this dependence does not hold at larger Q values. The mean relaxation time shows saturation, and this is an indication of a jump diffusion process in the liquid.¹³ In a jump diffusion process, the atoms become temporarily trapped in the cages formed by their neighboring atoms. When a cage breaks, the atom moves to its nearest neighboring cage. The time during which an atom stays in a cage is called the residence time. The jumping of

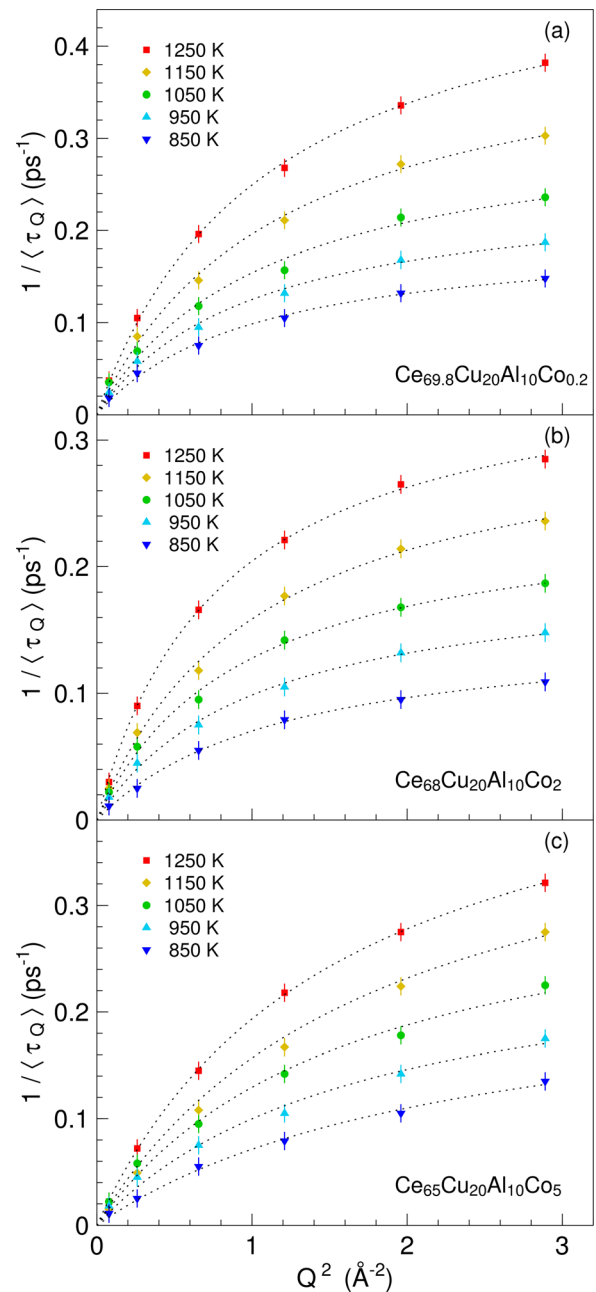


FIG. 2. The Q^2 dependence of inverse of the mean relaxation time of Cu atoms in: (a) $\text{Ce}_{69.8}\text{Cu}_{20}\text{Al}_{10}\text{Co}_{0.2}$, (b) $\text{Ce}_{68}\text{Cu}_{20}\text{Al}_{10}\text{Co}_2$, and (c) $\text{Ce}_{65}\text{Cu}_{20}\text{Al}_{10}\text{Co}_5$ liquids. The dotted lines are fits with the jump diffusion model (Eq. (2)).

atom from one cage to another gives rise to the long range diffusion process. It is believed that cage diffusion plays a crucial role in vitrification of glass-forming liquids.^{14,15}

The diffusion coefficient and residence time can be estimated from the Q^2 dependence of relaxation time as follows:

$$\frac{1}{\langle \tau_Q \rangle} = \frac{1}{\tau_0} \left[1 - \frac{1}{1 + DQ^2\tau_0} \right]. \quad (2)$$

Here, τ_0 and D are the residence time and diffusion coefficient, respectively.¹³ The residence times obtained from the fits are plotted in Fig. 3(a) as a function of temperature for all the alloy liquids studied. It is interesting to note that the residence time of Cu atoms in $\text{Ce}_{68}\text{Cu}_{20}\text{Al}_{10}\text{Co}_2$ is comparatively larger than in the other two alloy liquids. It was proposed that strong-bonding of the local structure induced by micro-alloying enhanced the GFA in these alloys.¹⁶ It was also shown that the observed sharp increase of GFA of this Ce based alloy upon Co addition is correlated with a dramatic increase of Al site symmetry.¹⁷ The strong bonding might also contribute to the increase in the residence time of Cu atoms in $\text{Ce}_{68}\text{Cu}_{20}\text{Al}_{10}\text{Co}_2$. On the other hand, the diffusion coefficients obtained from the fits (see Fig. 3(b)) show a systematic variation with the percentage of Co addition. At a given temperature, the diffusivity of Cu atoms decreases with the addition of Co; the 5% Co alloy melt shows the lowest and 0.2% Co alloy shows the highest diffusion coefficient

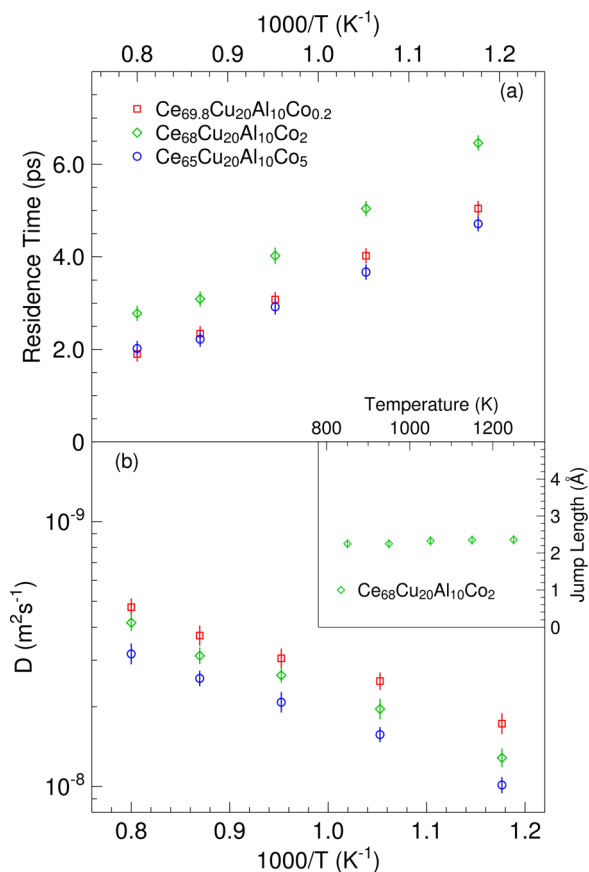


FIG. 3. (a) The residence time of Cu atoms in the three alloy liquids investigated plotted as a function of the inverse of temperature. (b) The self-diffusion coefficient of Cu atoms in the Ce based alloy liquids plotted as a function of the inverse of temperature. Inset: the temperature dependence of Cu jump length in $\text{Ce}_{68}\text{Cu}_{20}\text{Al}_{10}\text{Co}_2$ alloy liquid.

in the entire measured temperature range. Even though the diffusivity decreases with the higher percentage of Co, the residence time does not show composition dependence. This behavior might be due to the complex interplay of structural ordering and the back flow effect in the diffusion process in these liquids.¹⁸ This is an important observation since the GFA of the alloys is well correlated with the changes in the residence time (see Fig. 4). The vitrification occurs when the cage relaxation time increases dramatically on cooling a liquid, and the atoms do not get enough time for the long range motion to form a periodic structure. Consequently, atoms permanently trapped in their cage lead to the formation of amorphous structure.¹⁹ The atomic jump length can be calculated from the residence time and diffusion coefficient using the formula: $l = \sqrt{6D\tau_0}$, where l is the jump length, D is the diffusion constant, and τ_0 is the residence time. The jump length calculated for the $\text{Ce}_{68}\text{Cu}_{20}\text{Al}_{10}\text{Co}_2$ is plotted as a function of temperature in Fig. 3(b) (inset). The values of jump length were found to be of the order of $\sim 2.5 \text{\AA}$, which approximately corresponds to the interatomic distance in these alloy liquids. Recently developed theories based in the shear modulus or elastic model indicate a correlated variation of diffusivity with residence time.^{20–22} However, our results do not indicate a correlated variation as predicted by the theories. The reason for the uncorrelated variation of diffusivity with residence time might be due to the heterogeneous nature of relaxation dynamics present in our liquids. This is visible through the Q dependence of stretching exponents of self-correlation function of the liquids.

In conclusion, we have studied the atomic dynamics in $\text{Ce}_{69.8}\text{Cu}_{20}\text{Al}_{10}\text{Co}_{0.2}$, $\text{Ce}_{68}\text{Cu}_{20}\text{Al}_{10}\text{Co}_2$, and $\text{Ce}_{65}\text{Cu}_{20}\text{Al}_{10}\text{Co}_5$ using quasielastic neutron scattering. The self-correlation functions of Cu atoms in these alloy liquids, $\Phi(Q,t)$, exhibits stretching in time. The decay of the $\Phi(Q,t)$ can be well described with a *Kohlrausch–Williams–Watts* function. The stretching exponent evaluated from the KWW fits does not show a composition dependence. The atomic transport mechanism in these liquids has been identified from the momentum transfer dependence of the inverse of the mean relaxation times as a jump diffusion process. We have made an interesting observation that the composition dependence of the residence time of Cu atoms is strongly correlated with the GFA of the

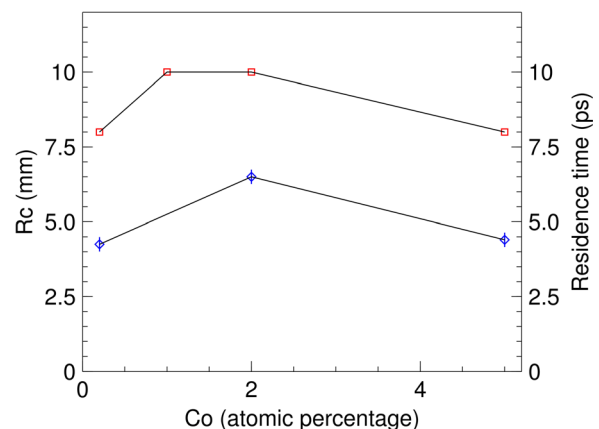


FIG. 4. The diamond symbols represent the residence times of Cu atoms in the alloy liquids. The square symbols indicate the critical casting thickness of $\text{Ce}_{70}\text{Cu}_{20}\text{Al}_{10}$ alloy as a function of Co addition (Ref. 4).

alloy liquids. The composition associated with the longest residence time corresponds to the enhanced GFA. However, the diffusivity of the Cu atoms was found to decrease monotonically with the increasing percentage of Co addition.

This project was financially supported by City University of Hong Kong research grant (Project No. 7004277). The neutron scattering experiment at Oak Ridge National Laboratory's (ORNL) Spallation Neutron Source was sponsored by the Scientific User Facilities Division, Office of Basic Energy Sciences, and U.S. Department of Energy. ORNL is managed by UT-Battelle, LLC, for the U.S. Department of Energy (DOE) under Contract No. DE-AC05-00OR22725.

¹X. P. Tang, U. Geyer, R. Busch, W. L. Johnson, and Y. Wu, *Nature* **402**, 160 (1999).

²Y. Q. Cheng and E. Ma, *Prog. Mater. Sci.* **56**, 379 (2011).

³D. Xu, B. Lohwongwatana, G. Duan, W. L. Johnson, and C. Garland, *Acta Mater.* **52**, 2621 (2004).

⁴B. Zhang, R. J. Wang, D. Q. Zhao, M. X. Pan, and W. H. Wang, *Phys. Rev. B* **73**, 092201 (2006).

⁵W. L. Johnson, *JOM* **54**, 40 (2002).

⁶A. Inoue, *Prog. Mater. Sci.* **43**, 365 (1998).

⁷G. Ehlers, A. Podlesnyak, J. L. Niedziela, E. B. Iverson, and P. E. Sokol, *Rev. Sci. Instrum.* **82**, 085108 (2011).

⁸F. Kargl, H. Weis, T. Unruh, and A. Meyer, *J. Phys.: Conf. Ser.* **340**, 012077 (2012).

⁹A. Meyer, *EPJ Web Conf.* **83**, 01002 (2015).

¹⁰S. M. Chathoth and A. Podlesnyak, *J. Appl. Phys.* **103**, 013509 (2008).

¹¹R. Böhmer, K. L. Ngai, C. A. Angell, and D. J. Plazek, *J. Chem. Phys.* **99**, 4201 (1993).

¹²S. M. Chathoth, B. Damaschke, J. P. Embs, and K. Samwer, *Appl. Phys. Lett.* **95**, 191907 (2009).

¹³K. S. Singwi and A. Sjolander, *Phys. Rev. B* **119**, 863 (1960).

¹⁴W. Kob and H. C. Andersen, *Phys. Rev. E* **48**, 4364 (1993).

¹⁵L. Larini, A. Ottochian, C. De Michele, and D. Leporini, *Nat. Phys.* **4**, 42 (2008).

¹⁶M. Chen, *NPG Asia Mater.* **3**, 82 (2011).

¹⁷X. K. Xi, L. L. Li, B. Zhang, W. H. Wang, and Y. Wu, *Phys. Rev. Lett.* **99**, 095501 (2007).

¹⁸K. Miyazaki, G. Srinivas, and B. Bagchi, *J. Chem. Phys.* **114**, 6276 (2001).

¹⁹W. Gotze, *Condens. Matter Phys.* **1**, 873 (1998).

²⁰J. C. Dyre and W. H. Wang, *J. Chem. Phys.* **136**, 224108 (2012).

²¹J. C. Dyre, *Rev. Mod. Phys.* **78**, 953 (2006).

²²F. Puosi and D. Leporini, *Eur. Phys. J. E* **38**, 87 (2015).